CLM - P 487

CLM - P 487

UKAEA

Preprint

TRAPPING OF ENERGETIC HYDROGEN IONS IN REACTIVE METALS

E S HOTSTON
G M McCRACKEN

CULHAM LABORATORY
Abingdon Oxfordshire

1977

CLM-P 487

TRAPPING OF ENERGETIC HYDROGEN IONS IN REACTIVE METALS

E S Hotston and G M McCracken
Applied Physics and Technology Division
Culham Laboratory, Abingdon, Oxfordshire, England
(Euratom/UKAEA Fusion Association)

ABSTRACT

A model is proposed to describe the trapping of a beam of energetic ions of hydrogen isotopes by targets of reactive metals in which the incident ions dissolve exothermically. The model considers the ions free to diffuse inside the metal, and to escape from the surface at a rate determined from the known solubility data.

It has been shown that in the case of semi-infinite geometry the trapping efficiency can be expressed in analytic form as a function of dose. However, in the two dimensional case appropriate for beam experiments, radial diffusion becomes important and a numerical solution has been found to be necessary. The model has been compared with experimental results on the trapping of 18 keV deuterons by targets of Nb, Zr, Ti and Pd in the temperature range 230-1000 K and in general good agreement has been obtained.

(To be published in Journal of Nuclear Materials)

May 1977

TRAPPING OF ENERGETIC HYDROGEN IONS IN REACTIVE METALS

E S Hotston and G M McCracken

1. INTRODUCTION

The trapping of hydrogen ions in metals has been studied for a number of years. It has been shown that of the ions incident on the target, a fraction are back-scattered and the rest are implanted in the metal. The probability of backscattering decreases with increasing energy and for a reduced energy[1,2,3] $\varepsilon = 5$ the back-scattering probability is < 10%. This paper is principally concerned with ions above this energy.

It has also been observed that the behaviour of the implanted ions is quite different in metals which react chemically with hydrogen and those which do not[1,4]. In the non-reactive metals, during hydrogen implantation the gas concentration builds up and diffuses to the surface where it desorbs. Eventually an equilibrium builds up between the incident flux and the desorbed flux, the time taken to reach equilibrium being a strong function of temperature. In the case of reactive metals it has been found that under some conditions the incident ion flux can be trapped with efficiency > 90% for doses up to the highest used experimentally ($\sim 10^{20}$ ions cm^{-2}). This has been explained qualitatively by showing that the activation energy for diffusion is less than the heat of solution of hydrogen in the metal, so that the gas atoms can diffuse into the solid without being able to jump the potential barrier at the surface. In the present paper we develop this model analytically and show that it gives good numerical agreement with experimental results.

2. THEORY

(i) The Model

When ions penetrate a solid they slow down by collisions with atoms and electrons and eventually stop, assuming the lattice temperature. Due to scattering, they have a range distribution which is approximately gaussian. In the lattice of many metals hydrogen atoms form a solid solution and are able to diffuse with a characteristic diffusion coefficient D of the usual form:

$$D = D_o \exp(-Q_2/RT) \qquad (1)$$

where Q_2 is the activation energy, D_o a constant and T is temperature.

The thermal release of hydrogen from the surface of a reactive metal has been shown to obey Sievert's Law[5] which states that the partial pressure, p, of a gas in equilibrium with a solution of gas, C(O,t), in the solid is given by:

$$p^{\frac{1}{2}} = A\ 10^2\ \frac{C(O,t)}{N}\ \exp\ (-Q_1/RT) \qquad (2)$$

where Q_1 is the heat of solution, N is the density of atoms in the target and A is a constant. Application of simple kinetic theory gives the rate of evolution of gas from the target per unit area to be:

$$F = B(T)\ C^2\ (o,t) \qquad (3)$$

where $$B(T) = 0.5 \cdot 10^{27}\ \alpha\ A^2 (MT)^{-\frac{1}{2}}\ N^{-2} \exp(-2Q_1/RT).$$

M is the atomic weight of the gas atom, and α is the sticking coefficient of the gas molecule at the surface. Because B(T) is proportional to $\alpha\ A^2$ the model does not distinguish between variations in α and variations in A which may occur between different specimens of the same material. We have assumed that the sticking coefficient is unity.

(ii) Plane Parallel Geometry

Consider a uniform flux of ions incident on the surface of a semi-infinite target for a time t, (a target will be effectively semi-infinite provided its thickness ℓ is much greater than $(Dt_1)^{\frac{1}{2}}$). The flow back out of the surface can be obtained by solving the one dimensional diffusion equation:

$$\frac{\partial C(z,t)}{\partial t} = D\ \frac{\partial^2 C(z,t)}{\partial z^2} \qquad (4)$$

subject to the appropriate boundary conditions. We assume that the initial concentration of gas is zero C(z,O) = O. At the surface of the target (z = o) conservation of particles gives the boundary condition:

$$J_o = B(T)C^2\ (O,t) - D\left(\frac{\partial c(z,t)}{\partial z}\right)_{z=o} \qquad (5)$$

where J_o is the incident particle flux density, assumed to be constant. The solution of equation (4) for the boundary conditions is:

$$C(0,t) = \frac{1}{\sqrt{D\pi}} \int_0^t F(t-\tau)\ \tau^{-\frac{1}{2}}\ d\tau \qquad (6)$$

where $F(t) = J_o - B(T)C^2(0,t)$ is the net flux of particles into the surface. It is required to obtain the reflection coefficient $R(t)$, where

$$R(t) = \frac{B(T)C^2(0,t)}{J_o} \qquad (7)$$

or the trapping coefficient $\eta = 1 - R(t)$.

A little manipulation of (6) gives:

$$\sqrt{R(t)} = \left(\frac{Q}{Q_c}\right)^{\frac{1}{2}} \left[1 - \int_0^t \frac{1}{2t^{\frac{1}{2}}}\ R(t-\tau)\ \frac{d\tau}{\tau^{\frac{1}{2}}}\right] \qquad (8)$$

where $Q = J_o t$ and $Q_c = D\pi/4B$.

This shows that there is a common curve relating $R(t)$ and Q/Q_c for all materials in which hydrogen obeys Sievert's Law. We may rewrite $R(t)$ in terms of $R(Q/Q_c)$ and obtain from (8) an approximate solution valid for $Q/Q_c \ll 1$ which is of the form:

$$R(Q/Q_c) = Q/Q_c \left[1 - \frac{2}{3}\left(\frac{Q}{Q_c}\right) + \frac{32}{45}\left(\frac{Q}{Q_c}\right)^2 - \frac{64}{315}\left(\frac{Q}{Q_c}\right)^3\right]^2 \qquad (9)$$

Equation (4) has also been integrated numerically and the results for the numerical integration and the approximate solution (equation 9) are compared in Figure 1. It is seen that equation (9) is valid for $Q/Q_c < 0.5$ with a relative error of less than 3%. The universal curve obtained can now be applied to any metal of interest simply by using the Sievert's Law constants and diffusion coefficients to obtain Q_c.

(iii) Cylindrical Geometry

The above result is not directly applicable to experiments with ion beams since the ion beam diameter is small compared to the size of the target in most cases. This situation can be analysed using cylindrical geometry. Let us define the ion beam radius to be $r = a$ and the target thickness $z = \ell$, Figure 2. We assume that the target radius is sufficiently large for there to be no appreciable diffusion to the circumference of the cylinder in the experimental time t_1, i.e:

$$Dt_1 \ll (R-a)^2 \qquad (10)$$

The concentration of the gas in the solid will be $C(r,z,t)$ and we have the boundary conditions $C(R,z,t) = 0$ from equation (10). The back surface of the target is assumed to be impermeable to the diffusing gas, so that:

$$\left[\frac{\partial C(r,z,t)}{\partial z}\right]_{r=\ell} = 0 \qquad (11)$$

As in the previous section, we have:

$$C(r,z,0) = 0 \qquad (12)$$

and

$$\left[D\,\frac{\partial C(r,z,t)}{\partial z}\right]_{z=0} = BC^2(r,0,t) \quad J(r)$$

where $B(T)$ is given by equation (3) and $J(r)$ is the flux density of the ions on the surface. The diffusion equation in cylindrical co-ordinates is:

$$\frac{1}{D}\,\frac{\partial C(r,zt)}{\partial t} = \frac{\partial^2}{\partial z^2}\,C(r,z,t) + \frac{1}{r}\,\frac{\partial}{\partial r}\left(r\,\frac{\partial C}{\partial r}\,(r,z,t)\right) \qquad (13)$$

The re-emission coefficient $R(t)$ and the trapping coefficient $\eta(t)$ are defined in a similar manner to the one dimensional case in section 2(ii).

$$R(t) = \frac{\int_0^R r\,BC^2(r,o,t)\,dr}{\int_0^R r\,J(r)\,dr}$$

and

$$\eta(t) = 1 - R(t)$$

The density profile across the beam is not always known precisely, so the calculation has been performed for three profiles of the form cos, $\cos^2$ and uniform, in each of which the total current was kept constant.

The diffusion equation (13) is solved numerically in a manner similar to that for the plane parallel case and the results are shown in Figure 3. A comparison is made between the results with and without radial diffusion which shows that radial diffusion plays an important role in experiments with finite beam diameters.

In what follows, a cosine density distribution will be assumed in the ion beam for the 2D calculations, and uniform current distribution will be assumed for the 1D models.

3. EXPERIMENTAL RESULTS

Measurements of the trapping efficiency over a wide range of temperatures have been made on a number of reactive metals, Ti, Zr, Nb, Er, Pd. The measurements were made with a mass separated beam of 18keV D^+ ions with current densities up to 0.7mA/cm^2. The target area bombarded was 0.07cm^2, and the target thickness was 1mm. Ultra high vacuum techniques were used throughout the accelerator, and the beam pressure in the target during these experiments was typically 5×10^{-9} torr, principally CO and H_2. The pressure rise due to the beam was $\lesssim 5 \times 10^{-8}$ torr.

The measurements were made by a partial pressure rise technique and absolute measurements obtained by comparison with a molybdenum target in which thermal desorption of the trapped ions had been studied[6]. Some of the results have been published previously[7]. Results for niobium, titanium and zirconium are shown in Figures 4, 5 and 6, together with the theoretical curves obtained by numerical solution of equation (13). The data used for Sievert's Law constants and diffusion constants is summarised in Table I. The diffusion data has been obtained mainly from the review of Volkl and Alefield[8].

4. DISCUSSION

(i) The theoretical calculations of the trapping coefficient as a function of time are in good agreement with the experimental results for niobium and zirconium at lower temperatures. In each case a correction has been made for those ions which are backscattered and thus not trapped in the target[2,3]. The calculations for titanium, while being of the right order of magnitude, are in less good agreement with experiment. This is probably due to the available data for diffusion and Sievert's Law constants in titanium being less reliable. There is disagreement between data from different sources. Moreover, the titanium hydrogen phase diagram is exceedingly complex[9] and it is possible that more than one phase exists even at low temperatures, thus invalidating the simple model.

At higher temperatures, both for niobium and zirconium, the shapes of the experimental curves alter, having a higher trapping coefficient at short times than the theory predicts. This effect is thought to be due to increased oxidation at high temperature and the oxide layer reducing the rate of diffusion out of the surface. Evidence of oxidation affecting trapping has also been observed by Bohdansky et al[4]. Under bombardment the oxide layer will be eroded and the diffusion rate increased to the theoretical value. Inclusion of such

a barrier in the theoretical model was found to give results very close to the experimental ones.

(ii) The experimental results have been plotted as a function of temperature at a fixed time of 1000 secs in Figure 7. It is seen that at these high doses the theoretical calculations are in very good agreement with the experiment. Two curves have been calculated for zirconium with different activation energies for diffusion; 6940 cals/mole and 8250 cals/mole. These two values are within the uncertainties in the published data[8].

(iii) Figure 8 shows the trapping efficiency of a niobium target after 1000s bombardment with ion beams of differing current densities. The target used in these experiments was not the same as that used for the results given in Figures 4 and 7. Reasonable agreement between experiment and model is obtained if it is assumed that the constant A is one half of the value used earlier. The temperature dependence of the trapping coefficient is strongly dependent upon the heat of solution Q_1 (see equation 3), and the model successfully predicts the observed temperature dependence with the same value of Q_1 as was used to compare theory and experiment in Figures 4 and 7. The need to use a different value for the pre-exponential constant A is thought to arise from a difference in the surface finish of the targets. Figure 8 also compares the results of the 1D and 2D models and shows the importance of radial diffusion in beam experiments. The semi-infinite 1D model allows the trapping coefficient to be expressed as a simple function of dose Q, the 2D model does not.

(iv) If diffusion was the dominant process in the trapping mechanism, palladium would also be a highly absorbing target. However, Table 1 shows that the heat of solution Q_1 for palladium is much less than for the other metals, in fact less than one half the activation energy for diffusion. The parameter $Q_c = D\pi/4B$ introduced in equation 9, is a useful guide to the dose that can be received before the trapping coefficient departs significantly from unity. A comparison of Q_c for palladium and titanium shows that palladium is a much less efficient trapping medium than titanium by several orders of magnitude, Table II. The trapping efficiency of palladium increases with temperature because the coefficient D increases with temperature more rapidly than does the coefficient B.

Experiments with a palladium target, using deuteron beams comparable to those used with the other metals, at temperatures in the range 230K-270K, showed that the trapping was negligible after a few seconds bombardment. This time is comparable with the time constants of the apparatus.

(v) There have been many investigations of the solubility of hydrogen in metals which indicates that Sievert's Law is only obeyed up to concentrations of about 10%[10]. Thus, if the model predicts concentrations in excess of 10% it is invalid. Figure 7 indicates the maximum concentrations of the dissolved gas at the centre of the focal spot of the ion beam; they do not exceed 2.7% so that the model is valid.
In general, the dose that can be accepted by a target at a given temperature before the concentration rises to a level at which the model becomes invalid, decreases as the beam current increases. This applies not only to 2D models but also to the semi-infinite 1-D model, so that great care must be taken in scaling from the results of beam experiments.

(vi) Figure 7 shows that metals with a large heat of solution trap better at high temperatures. Thus, for high temperature operation, zirconium and the rare earths are the obvious choice. However, in order to trap beams with high current densities, it would be better to choose metals with diffusion coefficients so that the trapped hydrogen would diffuse rapidly into the bulk. In this respect, vanadium, niobium and tantalum should be better. Unfortunately however, high current densities result in high power loadings and hence a rise in surface temperature. Operating Nb or V at high power loading would probably require a coolant operating well below room temperature. There is thus no obvious "best" trapping material and the choice will have to be made for each particular application.

(vii) When the diffusion coefficient is low, for example at low temperatures, the concentration will build up at a rate determined only by the range and range distribution of the incident ions in the metal. Experimentally it is found that a certain critical dose is required before the trapping coefficient begins to fall significantly below unity. Then it decreases exponentially consistent with ion induced de-trapping of previously trapped ions. The critical dose may be related to the dose required to reach the stoichometric hydride ratio below which the hydrogen is tightly bound. The cross section for ion induced detrapping at higher concentrations is the same within a factor 2 for all the metals measured and is $\sim 1 \times 10^{-18}$ cm^2 at 18 keV.

(viii) There are other considerations to be taken into account, in deciding which material to choose for high trapping efficiencies. The trapping effect we have been discussing is only applicable if the incident ion slows down in the metal. We have already mentioned than an ion can be backscattered by multiple collisions in the lattice before slowing down to thermal energies. This probability can be calculated on the Lindhard theory[3] and it has been shown that the theory is in quite good agreement with experiment. The results indicate that the probability of back scattering decreases with incident ion energy and increases with target atomic number. At 1 keV for example, the probability of backscattering is ∿20% for Ti, ∿30% for Zr and ∿40% for Er[2,11]. Thus at low energies, consideration of the backscattering could be an important factor in choosing the trapping material. A further factor at low energy has been demonstrated by Bohdansky et al[4]. The metals which are good trapping materials are in general highly reactive and oxide coatings are commonly formed even under high vacuum. If the range of the incident ion is less than the thickness of the oxide coating, then the trapped ion will not experience either the high heat of solution or the high diffusion coefficient of the metal and trapping will not occur at high doses. Apart from this factor, the probability of trapping should be independent of the incident ion energy, provided that the ions slow down in the metal, i.e. provided the backscattered fraction has been taken into account.

(ix) The good agreement of this diffusion model with the experimental results is a little surprising at first, as attempts to make an analogous model for unreactive metals failed to give the results expected on the basis of thermal diffusion[12]. This was shown to be due to trapping of the diffusing atoms at damage sites in the lattice[13]. The most probable explanation why trapping sites are not important in the present model is that the diffusive flow is predominantly into the bulk. The potential barrier restricts diffusion out of the surface and the surface concentration is determined by the in-diffusion. The region subject to radiation damage is about 2000Å deep for the 18keV ions used and is thus small compared with the total diffusive path into the bulk.

5. CONCLUSIONS

A model of the trapping of hydrogen in reactive metals has been analysed in detail. Calculations of the trapping efficiency as a function both of dose and

of target temperature agree well with those which have been determined experimentally. The trapping behaviour is dependent primarily on the diffusion coefficient and the heat of solution of hydrogen in the metal. The theoretical model makes clear that the current density is important and that the results for beams are dependent on radial diffusion of the hydrogen away from the point of implantation as well as diffusion along the axis into the solid. Thus the results of beam experiments must not be applied directly to conditions where the incident flux has a large cross-sectional area. Such cases include many plasma physics devices e.g. at the target of a divertor and perhaps also the case of dumping of very high current ion beams from extended sources. In this situation the plane parallel geometry analysed in section 2 should be applicable.

For plane parallel geometry an approximate analytical solution has been derived which shows that a universal curve exists which is applicable to cases in which Sievert's Law applies and in which there is a simple non-concentration dependent diffusion coefficient.

The model described breaks down at high concentrations where Sievert's Law no longer holds, but the point at which the calculations are no longer accurate is readily predicted from the model for any particular system.

ACKNOWLEDGEMENT

We are grateful to D K Jefferies for his assistance in making the experimental measurements.

REFERENCES

1. McCracken, G.M. Rept Progs Phys 38, p241, 1975.
2. Behrisch, R. To be published in J de Physique, April 1977.
3. Oen, O.S. and Robinson, M.T. Nucl Inst and Methods 132, p647, 1976.
4. Bohdansky, J., Roth, J., Sinha, M.K. and Ottenberger, W. Surface Effects on Controlled Fusion Devices. Proceedings 2nd Conference on Surface Effects in Controlled Fusion Devices, San Francisco, 1976, p115. North Holland 1977.
5. Dushman, S. Scientific Foundations of Vacuum Technique, 2nd Edition, Chapter 8, Wiley 1962.
6. McCracken, G.M. and Maple, J.H.C. Brit Jnl App Phys 18, p914, 1967.
7. McCracken, G.M., Jefferies, D.K. and Goldsmith, P. Proceedings 4th Int. Vac Congress, Inst of Physics Conf Series 5, p149, 1968.
8. Völkl, J. and Alefeld, G. Diffusion in Solids, Recent Advances. Ed Nowick, A. and Burton, J. Chapter 5, p231, Academic Press 1975.
9. Hansen, M. Constitution of Binary Alloys, p799, McGraw Hall 1958.
10. Smithells, C.J. Metals Reference Book, 4th Edition, Vol II, p605.
11. McCracken, G.M. Proc Int Symp on Plasma Wall Interactions, Julich 1976. To be published by Euratom.
12. Erents, S.K. and McCracken, G.M. J Phys D 2, p1397, 1969.
13. McCracken, G.M. and Erents, S.K. Proc Int Conf on Applications of Ion Implantation to Metals, Albuquerque, p585. Plenum Press 1973.
14. Poulter, K and Pryde, J.A. Chemical Communications, p939, 1967.
15. Wasilensky, R.J. and Kehl, G.M. Metallurgia, 50, p225, 1954.
16. Sof'ina, V.V. and Pavlovskaya, N.G. Russian Jnl Phys Chem, 34, p525. 1960.
17. McQuillan, A.D. Proc Roy Soc 204A, p309, 1950.
18. Morton, J.R. and Stark, D.S. Trans Faraday Soc 56, p354, 1960.
19. Temple, C.R. Editor, Nuclear Reactor Handbook, 2nd Edition, 1, 1730, Interscience 1960.
20. Mallet, M.W. and Albrecht, W.M. Jnl Electrochemical Soc 104, p142, 1957.
21. Gulbransen, E.A. and Andrew, K.F. Jnl Electrochemical Soc 101, p560, 1960.
22. Lacher, J.R. Cited in reference 5 above.

Table 1. Selected Solubility and Diffusion Constants

Metal	Gas	D_o cm^2s^{-1}	Q_2 cal/g mol	Ref	A $torr^{\frac{1}{2}}$	Q_1 cal/g atom	Ref
Nb	H	0.0005	2430	8	395	8600	14
	D	0.00054	2966	8			
Ti	H	0.018	12400	15	4.5	9400	16
					98	10800	17
					106	11300	18
Zr	H	0.00047	5940	19	181	14500	16
		0.00066	7060	20			
		0.0011	11500	21			
	D	0.00073	11500	21	192	14450	18
Pd	H	0.0029	5288	8	93.4	2040	22

Values Used in Present Work

Metal	Gas	D_o cm^2s^{-1}	Q_2 cal/g mol	A $torr^{\frac{1}{2}}$	Q_1 cal/g atom
Nb	D	0.00054	2966	395*	8600*
Ti	D	0.0127*	12400*	106	11300
Zr	D	0.00047*	8250*	192	14500
		0.00047	6940		
Pd	D	0.00205*	5288*	93.4	2040

*Values inferred from results for Hydrogen

TABLE II

Comparison of $Q_c = D\pi/4B$ for Pd and Ti

TK	300	1000	
Pd	$1.68 \cdot 10^{12}$	$4.27 \cdot 10^{13}$	D^+cm^{-2}
Ti	$3.94 \cdot 10^{21}$	$4.50 \cdot 10^{16}$	D^+cm^{-2}

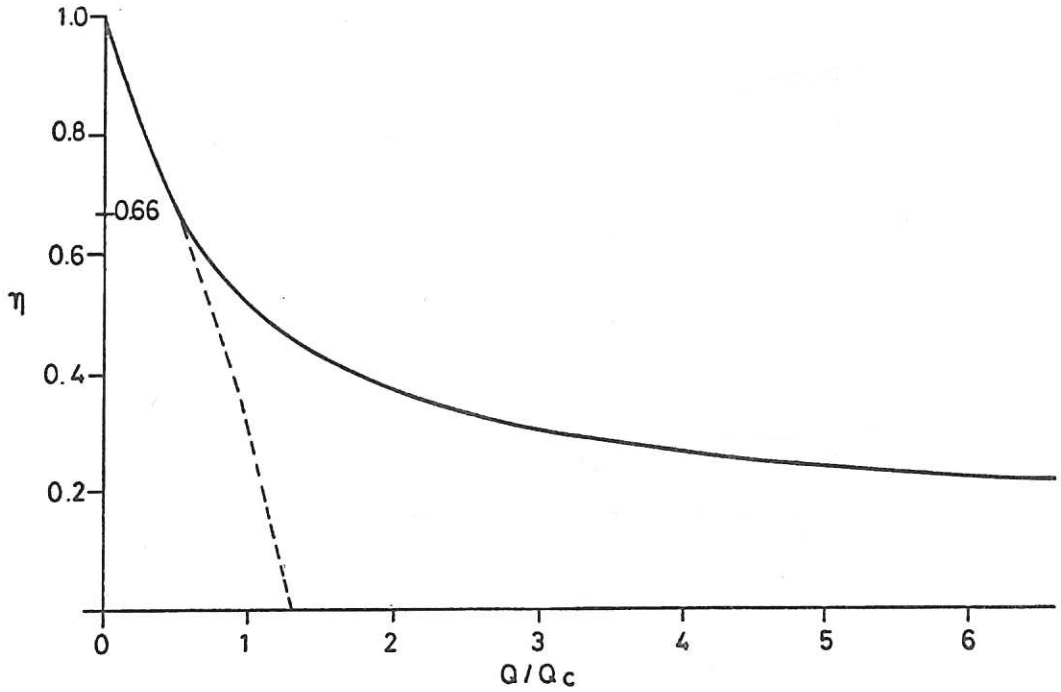

Fig.1 Trapping coefficient η as a function of normalized dose Q/Q_c for a uniform beam incident upon a semi-infinite target. Q_c depends upon the diffusion coefficient and the heat of solution of the trapped ion in the metal surface (equation 8). The solid line is the numerical solution of equation 8 and the broken line is the analytical solution valid for $Q/Q_c \ll 1$ obtained from equation 9.

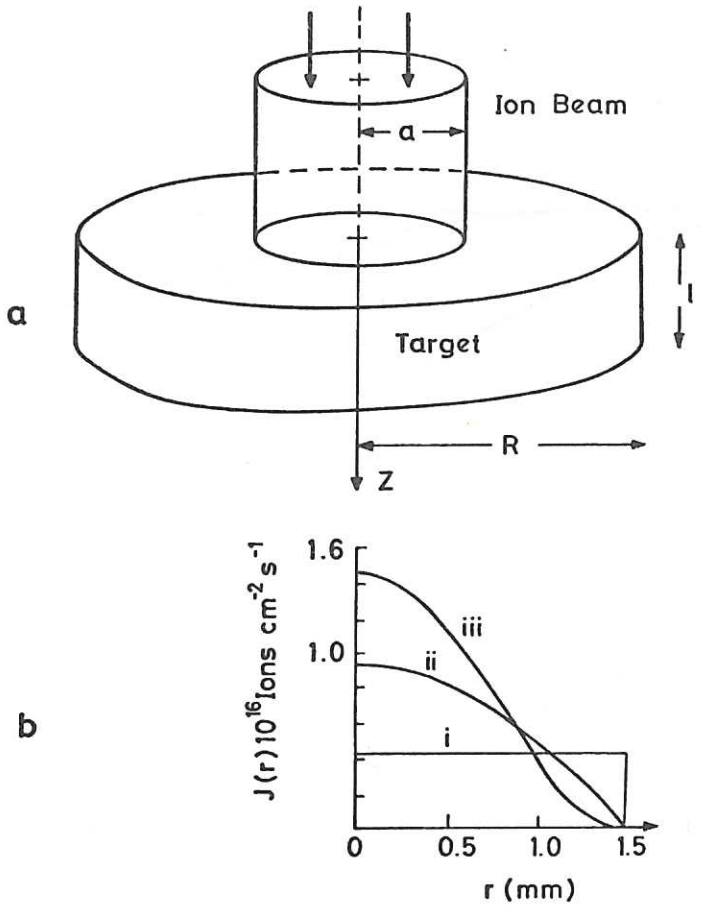

Fig.2 (a) Illustrating the geometry of the cylindrical model. (b) The flux density distribution across a 50 μA ion beam 3 mm diameter. (i) Uniform current density. (ii) Cosine current density. (iii) Cosine squared current density.

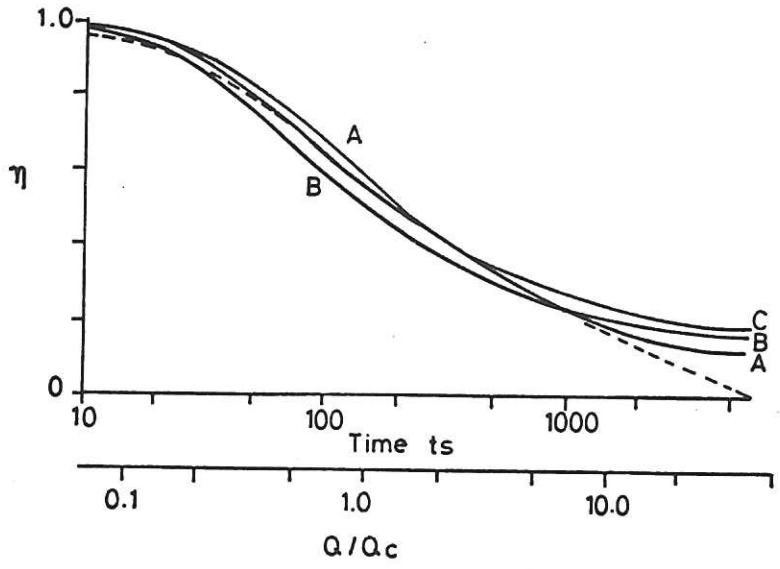

Fig.3 Trapping coefficient η calculated for a 50 μA D^+ beam 3 mm diameter incident upon a Zr target 1 mm thick at a temperature of 800 K. A – uniform current distribution. B – cosine square current distribution. C – cosine current distribution. The broken line is for uniform current distribution with no radial diffusion.
D_o = 0.00047 $cm^2 s^{-1}$. $Aa^{1/2}$ = 192 $torr^{1/2}$. Q_2 = 8250 cal $mole^{-1}$. Q_1 = 14500 cal gm $atom^{-1}$.

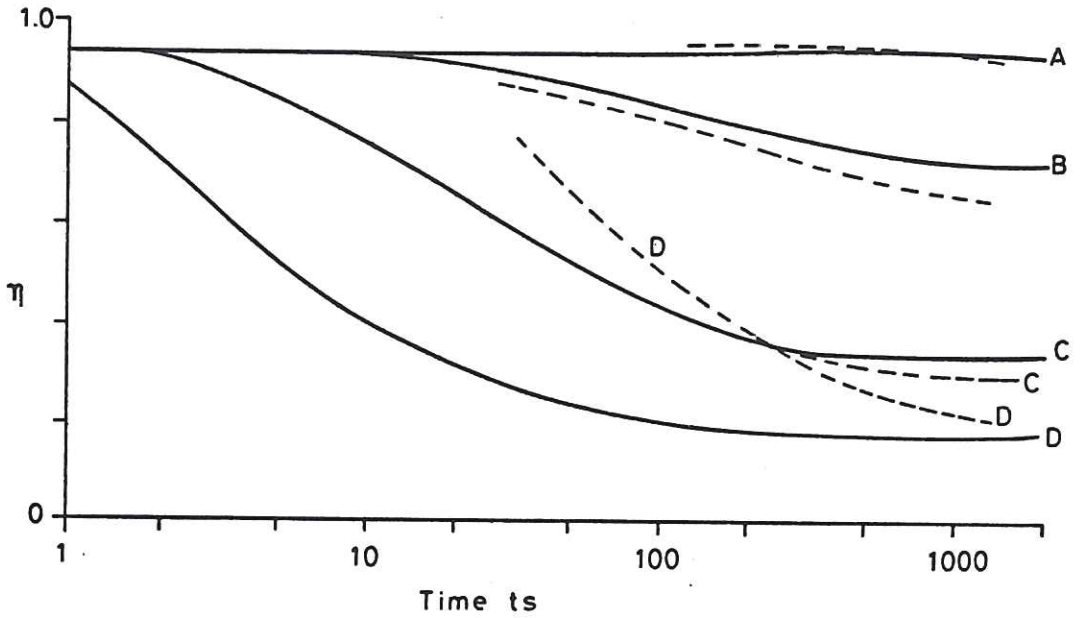

Fig.4 Trapping efficiency η as a function of time for niobium target bombarded with 18 keV D^+. Broken lines experimental results. Solid lines predictions of theory, a fraction of 0.06 of the incident beam is assumed to be backscattered.

	A	B	C	D
$I_b(\mu A)$	45	52	52	47
T(K)	335	452	563	681

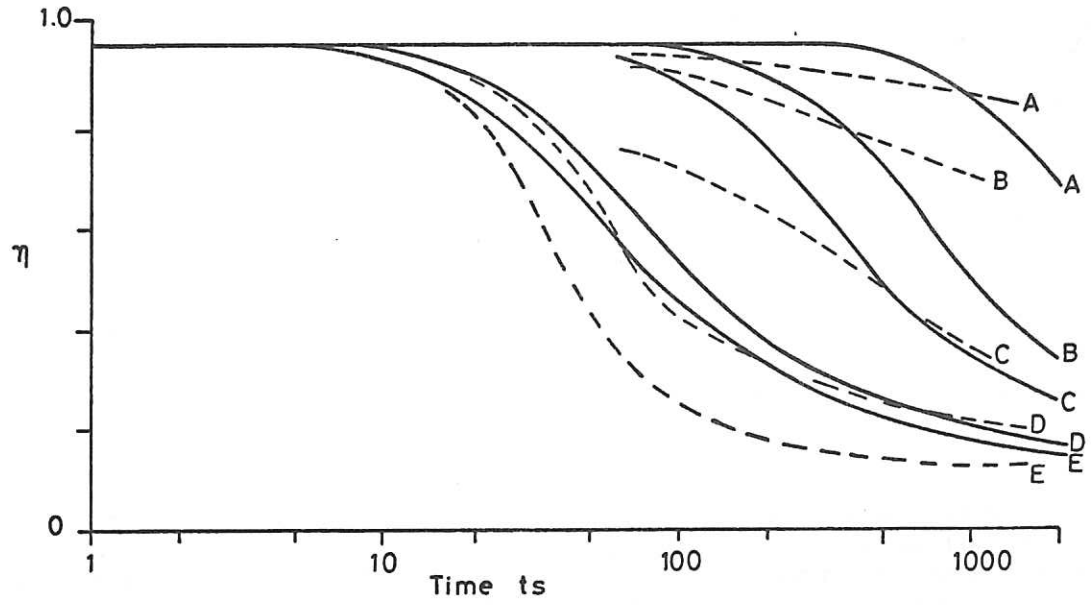

Fig.5 Trapping coefficient η as a function of time for a titanium target bombarded with 18keV D^+. Broken lines experimental results. Solid lines predictions of theory, a fraction of 0.03 of the incident beam is assumed to be backscattered.

	A	B	C	D	E
$I_b(\mu A)$	40	51	51	46	49
T(K)	477	531	574	699	728

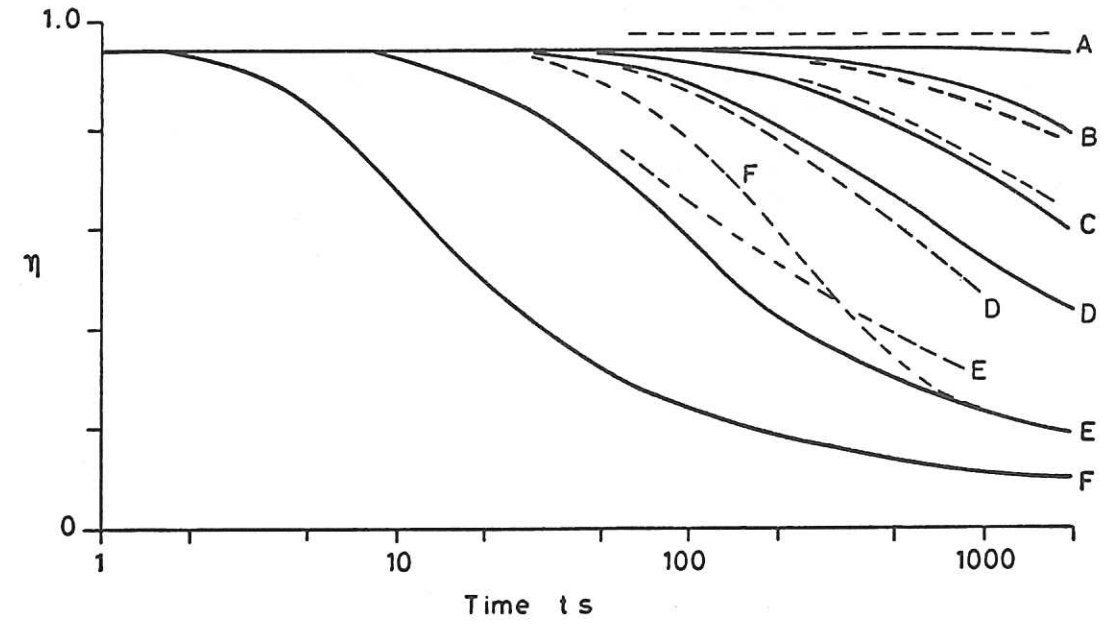

Fig.6 Trapping coefficient η as a function of time for a zirconium target bombarded with 18keV D^+. Broken lines experimental results. Solid lines predictions of theory, a fraction 0.06 of the incident beam is assumed to be backscattered. Q_2 the activation energy for diffusion is assumed to be 8250 cal $mole^{-1}$.

	A	B	C	D	E	F
$I_b(\mu A)$	54	52	47	47	59	49
T(K)	477	598	653	699	812	988

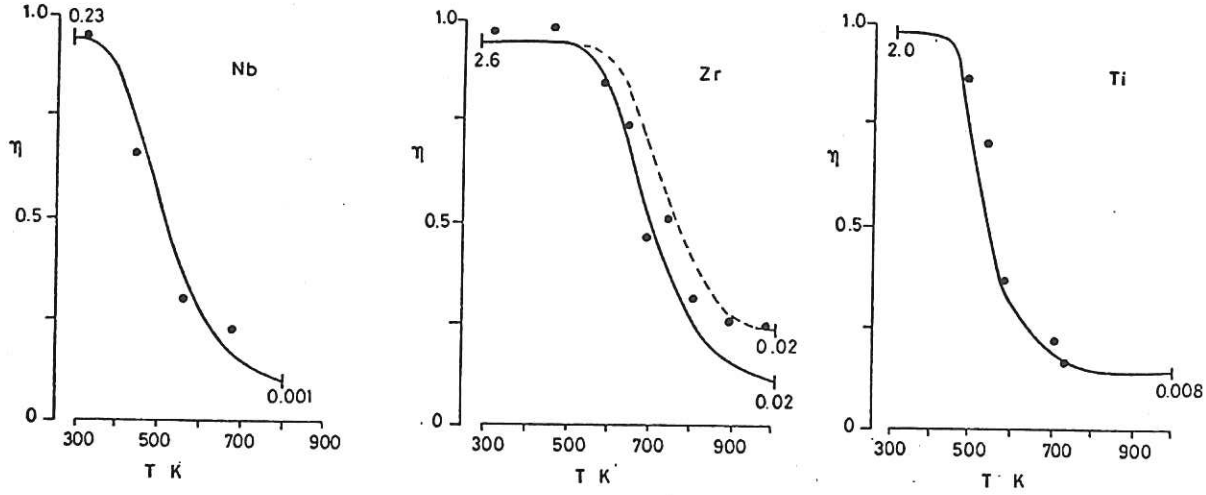

Fig.7 Trapping coefficient for Nb, Zr, Ti targets bombarded with a 50μA (0.7 mA cm^{-2}) beam of 18keV D^+ for 1000s as a function of temperature. The numericals alongside the curves give the atomic concentration of the trapped ions at the centre of the focal spot. The solid curve for Zr is for a value of Q_2 = 8250 cal mole^{-1} and the broken line for Q_2 = 6940 cal mole^{-1}. The experimental points are for a nominal current of 50μA.

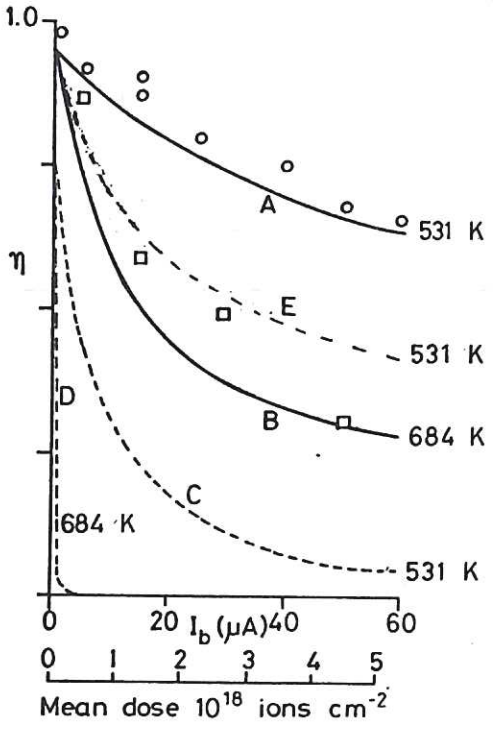

Fig.8 Trapping coefficient η for a niobium target 1 mm thick bombarded for 1000s with an 18keV D^+ beam of intensity I_b. The curves are:

A,B	2–D model	$Aa^{1/2}$ = 197.5 torr$^{1/2}$	○ Experimental points 531 K
C,D	1–D model	$Aa^{1/2}$ = 197.5 torr$^{1/2}$	□ Experimental points 684 K
E	2–D model	$Aa^{1/2}$ = 395 torr$^{1/2}$	